Aberration-corrected Czerny–Turner imaging spectrometer with a wide spectral region

Qingsheng Xue,[1,2] Shurong Wang,[1,*] and Fengqin Lu[3]

[1]State Key Laboratory of Applied Optics, Changchun Institute of Optics, Fine Mechanics and Physics, Chinese Academy of Sciences, Changchun, Jilin 130033, China

[2]Graduate School of the Chinese Academy of Sciences, Beijing 100039, China

[3]College of Science, University of Shanghai for Science and Technology, Shanghai 200093, China

*Corresponding author: wsr_608@yahoo.com.cn

Received 19 September 2008; revised 3 November 2008; accepted 11 November 2008; posted 14 November 2008 (Doc. ID 101720); published 15 December 2008

A modified asymmetrical Czerny–Turner arrangement with a fixed plane grating is proposed to correct aberrations over a wide spectral region by analysis of the dependence of aberration correction for different wavelengths. The principle and method of aberration correction are described in detail. We compare the performance of this modified Czerny–Turner arrangement with that of the existing Czerny–Turner arrangement by using a practical Czerny–Turner imaging spectrometer example. © 2009 Optical Society of America

OCIS codes: 300.0300, 300.6190, 120.4570, 120.0120, 120.0280.

1. Introduction

The Czerny–Turner spectrograph has been studied and applied by some authors [1,2] both in its classical form (spherical mirrors and symmetrical design) and with different modifications. Several Czerny–Turner spectrographs using multielement detectors have flown in space, e.g., the Middle Atmosphere High Resolution Spectrograph Investigation (MAHRSI) [3] and Shuttle Ozone Limb Sounding Experiment-2 (SOLSE-2) [4]. The MAHRSI utilized a scanned grating with the wavelength region from 190 to 320 nm. The grating must be scanned to cover the entire spectral range of the instrument. The SOLSE-2 demonstrated the feasibility of using charge-coupled device (CCD) technology to eliminate moving parts in simpler, cheaper, ozone-mapping instruments. The SOLSE-2 permitted simultaneous acquisition of a multiwavelength image from 275 to 425 nm. It is remarkable that, in all the existing Czerny–Turner arrangements, the grating is placed in the vicinity of the focal plane of the mirrors. For these positions of the grating, the aberrations depend on the wavelength substantially and, therefore, the useful spectral range decreases considerably. However, some optical spectroscopic measurement and remote-sensing applications (e.g., thermospheric/ionospheric studies [5] and limb scattering measurements [6]) require simultaneously obtaining a multiwavelength image over a wider spectral region (e.g., 280 to 680 nm) with a fixed dispersive element. When the aberrations are corrected for the central wavelength, distorted or elongated slit images are formed for marginal wavelengths with existing Czerny–Turner arrangements. This possibly leads to misunderstanding of the spectra and image. Thus, the existing Czerny–Turner spectrograph cannot fulfill the requirements. Therefore, we study the optical design of the Czerny–Turner imaging spectrometer to correct the aberrations over a wide spectral region with a fixed grating (not a scanned grating).

Here a Czerny–Turner arrangement is given by taking into consideration the dependence of aberration correction for different wavelengths. It is confirmed that the aberration-corrected arrangement

0003-6935/09/010011-06$15.00/0

found here is better than the existing arrangement. The principle and method of aberration correction are described in Section 2. An illustrative example is given in Section 3.

2. Principle and Method of Aberration Correction

A. Spherical Aberration

A concave spherical mirror has a spherical aberration when used on axis. If used off axis, in addition to the spherical aberration, it has coma, astigmatism, field curvature, and distortion. In most cases, only the first three aberrations are important. A concave spherical mirror's focal length and aperture are dependent on the system's relative aperture and the system's aberration allowance. A bigger relative aperture enhances the system's ability to collect light, making the spectrometer more sensitive to low-power light. But this will increase the system's spherical aberration and stray light and introduce more coma and astigmatism, which lead to the decrease of imaging spectrum's quality and the system's spectral resolution. On the other hand, if the relative aperture is too small, the system cannot get enough incident light power.

In the beginning of the design, a spherical mirror's aberration and Rayleigh criterion are introduced as the design criteria of the relative aperture. The system's F-number is represented as $F\# = f/D$, where D represents the diameter of the mirror. W_S is the wavefront aberration due to spherical aberration, as shown in Eq. (1):

$$W_{S(\max)} = \frac{(y_{\max})^4}{8r^3}. \tag{1}$$

According to the Rayleigh criterion, we derive the following equation:

$$\frac{(y_{\max})^4}{8r^3} \le \frac{\lambda}{4}. \tag{2}$$

In Eq. (2), r represents the radius of curvature of the spherical mirror, which equals $2f$, and $y_{\max}$ is the half-aperture of the spherical mirror, $D/2$. Equation (2) can be rewritten in the form

$$f \le 256 \cdot \lambda \cdot (F\#)^4, \tag{3a}$$

$$D \le 256 \cdot \lambda \cdot (F\#)^3. \tag{3b}$$

As has been discussed so far, the system's aberration allowance, incident light power, and detecting system should be considered to determine the system's relative aperture.

B. Coma Aberration

A spectrometer based on the asymmetrical Czerny–Turner configuration consists of a grating, a collimating mirror, and a focusing mirror. Coma aberration was corrected on the basis of the Shafer equation, which can be expressed as follows [7]:

$$\frac{\sin\alpha_1}{\sin\alpha_2} = \left(\frac{r_1}{r_2}\right)^2 \left(\frac{\cos\theta\cos\alpha_1}{\cos i\cos\alpha_2}\right)^3. \tag{4}$$

Here, α_1, α_2 are the off-axis incident angles for the central ray on the collimating and condensing mirrors, i and θ are the incident and diffraction angles on the grating, and r_1 and r_2 are the radii of curvature of the collimating and focusing mirrors. By replacing the third-order terms in α_1 (typically, 5°–8°) and α_2 (approximately 10°) as $\cos^3\alpha_1$ and $\cos^3\alpha_2 \approx 1$, one can obtain the approximate relation

$$\frac{\sin\alpha_1}{\sin\alpha_2} = \left(\frac{r_1}{r_2}\right)^2 \left(\frac{\cos\theta}{\cos i}\right)^3. \tag{5}$$

Thus we can eliminate the coma aberration by adjusting the incident α_1 and α_2 and curvatures r_1 and r_2 to fulfill Eqs. (4) and (5). As is known, the spectral profile is asymmetrically deformed by the coma aberration, whereas the spherical aberration symmetrically expands the width. For a Czerny–Turner imaging spectrometer, α_2 may not be considered large enough to avoid obscuration. To make α_1 as small as possible, we set $r_2 > r_1$ based on Eq. (5). So we decide to optimize the incident angle to the collimating mirror for a fixed focusing mirror, where i and θ are determined by the groove interval and the geometric configuration of the grating based on Eq. (6):

$$d(\sin i + \sin\theta) = m\lambda. \tag{6}$$

Here, d is the groove interval and m is an integer that represents the spectral level.

C. Astigmatism

The next step is to correct an astigmatism that extends an image to several millimeters along the slit height (sagittal direction) owing to the different focal lengths of the mirrors for the tangential and the sagittal directions. The astigmatism can be corrected by use of a toroidal mirror that possesses a distinct focal length along the tangential and the sagittal directions. Moreover, a toroidal mirror is particularly simple to make in comparison with other nonspherical surfaces. The focal distance to the tangential image for a collimating beam reflected from a spherical surface is [8]

$$f_{tn} = (r_n/2)\cos\alpha_n + \Delta f_{tn}; \tag{7}$$

the focal distance to the sagittal image is

$$f_{sn} = (\rho_n/2)\sec\alpha_n + \Delta f_{sn}. \tag{8}$$

Here, $n = 1$ and 2, denoting the collimating and focusing mirrors. In Eqs. (7) and (8), $f_{t,s}$ is the distance measured along a principal ray from the image plane

to the mirror surface, α is the off-axis angle of the ray, the Δf is the small distances added to the third-order approximation ($\Delta f_t \approx \Delta f_s$), r is the radius of curvature of the mirror in the tangential plane, and ρ is the radius of curvature in the sagittal plane. If $r = \rho$, the surface is a sphere. Rays in the sagittal (vertical) plane focus at a longer distance than rays in the tangential (horizontal) plane. The astigmatism is accumulated in collimating and focusing mirrors. For instance, the extended focal length along the sagittal directions is given by

$$\delta f = (f_{s1} - f_{t1}) + (f_{s2} - f_{t2}). \tag{9}$$

The extended image along the sagittal plane is corrected by a shorter focal length compared with that for the tangential plane for the focusing mirror.

D. Aberrations Over a Wide Spectral Region

The astigmatism does not depend on wavelength but, rather, on the incident angles to the mirrors, as given by Eqs. (7) and (8). However, the optimum angle of incidence to correct coma aberration is dependent on the incident and the diffraction angles and, therefore, is substantially related to the wavelength. Note that the coma and astigmatism are corrected by adjustment of the incident angle α_1 and focal length of f_{s2}, which are implicitly correlated. The incident angles to the focusing mirror are different for different wavelengths because of the different diffractive directions at the grating. It seems that one cannot correct the aberrations for different wavelengths at the same time because they have distinct optimum conditions that are due to different incident angles to the focusing mirror. However, the aberrations for different wavelengths can be corrected by the same optical parameters if the incident angles (α_2) for different wavelengths to the focusing mirror are adjusted to be approximately identical by adoption of a particular arrangement. We find the arrangement by geometric analysis as follows.

We find that only when the position of the grating is coplanar with the center of curvature of the focusing mirror (i.e., the distance $L_{\text{g-fc}}$ between the grating and the focusing mirror is equal to $2f_{t2} = r_2 \cos\alpha_2$) are the incident angles for different wavelengths approximately identical. Thus, the aberrations can be simultaneously corrected by the same optical parameters for different wavelengths. As shown in Fig. 1(a), the center of curvature of the focusing mirror is located at point C ($x = 0$, $y = 0$). The points O (r_2, 0) and G ($r_2 \sin^2\alpha_2$, $r_2 \sin\alpha_2 \cos\alpha_2$) are the centers of the focusing mirror and of the grating, respectively, with a distance of $L_{\text{g-fc}} = 2f_{t2} = r_2 \cos\alpha_2$. The rays for different wavelengths proceed along the different light paths. The light paths G–O or G–A, and G–B are for the central wavelength λc, λc-$\Delta\lambda$, and $\lambda c + \Delta\lambda$, respectively, where $A = A(x, y)$ and $B = B(x, -y)$. $\pm\Delta\omega$ is the deviation angle owing to a different wavelength from the central wavelength. It must be proved that the incident angles for wavelengths λc-$\Delta\lambda$ and $\lambda c + \Delta\lambda$, $\angle$GAC and $\angle$GBC are approximately in accordance with that for central wavelength $\angle$GOC only for $L_{\text{g-fc}} = 2f_{t2} = r_2 \cos\alpha_2$. Based on sine theorem, we can derive the relations

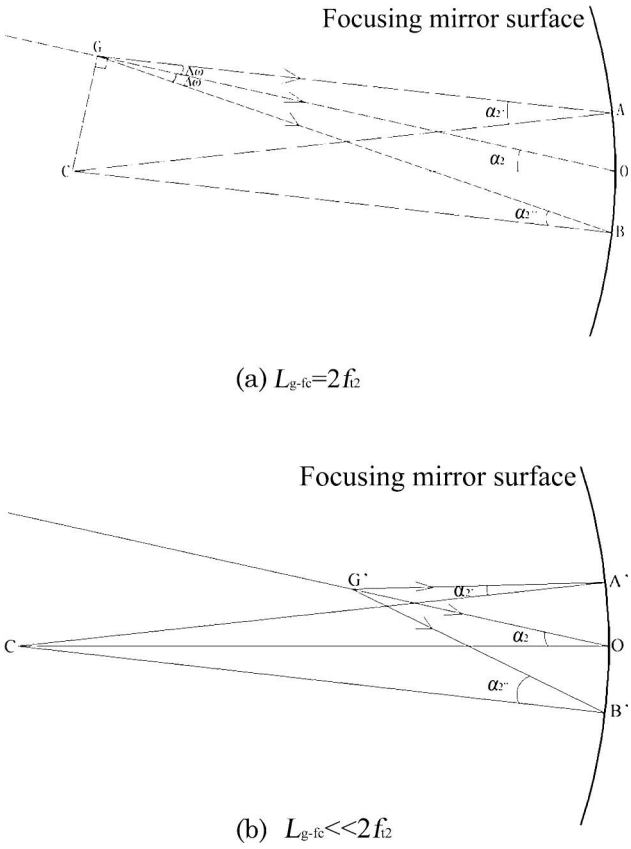

Fig. 1. Geometric relation between the distance $L_{\text{g-fc}}$ and the incident angles to the focusing mirror for different wavelength.

$$\frac{|GC|}{\sin\angle GAC} = \frac{|CA|}{\sin\angle CGA} = \frac{r_2}{\sin\left(\frac{\pi}{2} + \Delta\omega\right)} = \frac{r_2}{\cos\Delta\omega}, \tag{10}$$

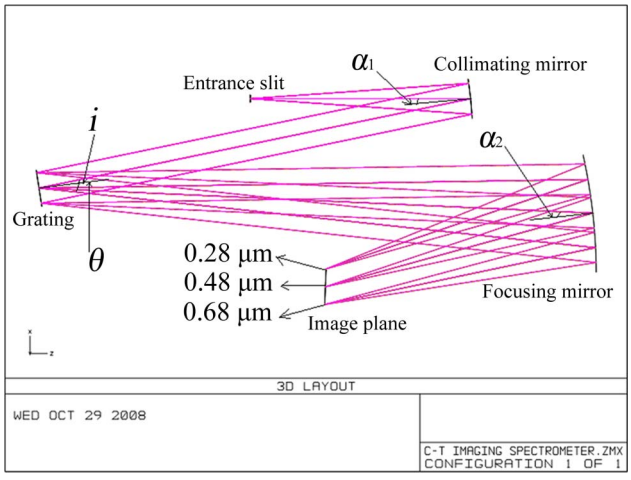

Fig. 2. (Color online) Layout of the Czerny–Turner imaging spectrometer system.

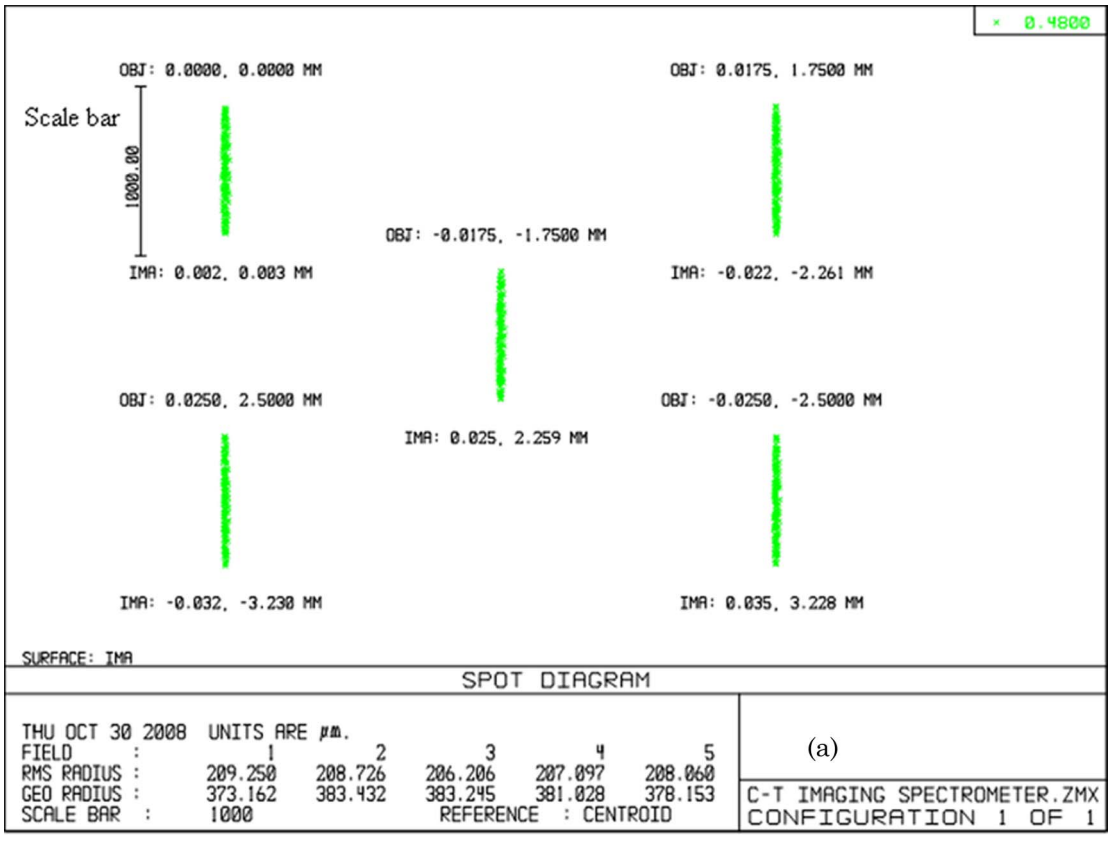

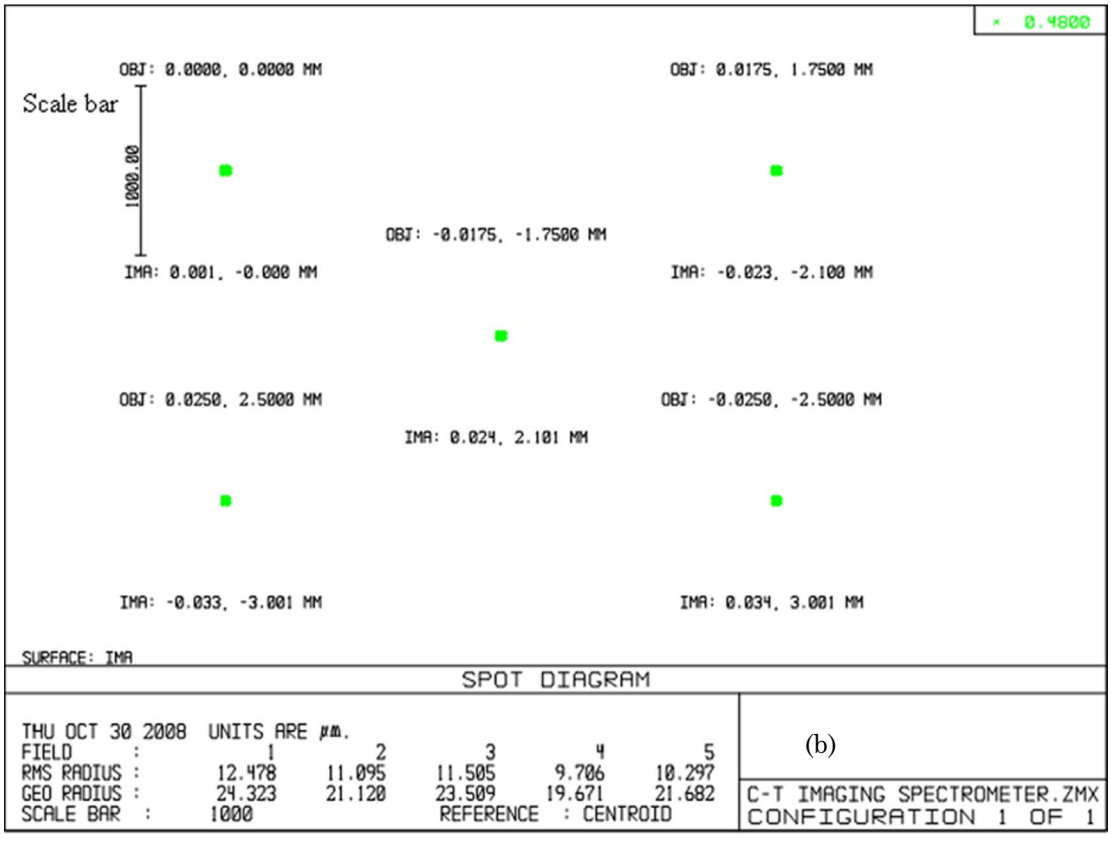

Fig. 3. (Color online) Spot diagrams for different fields of view with (a) a spherical and (b) a toroidal focusing mirror.

$$\frac{|\mathrm{GC}|}{\sin\angle\mathrm{GOC}} = \frac{|\mathrm{CO}|}{\sin\angle\mathrm{CGO}} = \frac{r_2}{\sin\left(\frac{\pi}{2}\right)} = r_2. \qquad (11)$$

Thus, $\sin\angle\mathrm{GAC} = \sin\angle\mathrm{GOC}\cos(\Delta\omega)$. Because $\Delta\omega \approx 0$, so $\angle\mathrm{GAC} = \alpha_{2'} = \angle\mathrm{GOC} = \alpha_2$. (We will not repeat the derivation from B, as the same mathematics can be used.) This relation does not depend on α_2, but is ensured by $\Delta\omega \approx 0$. Therefore, one can anticipate the same situation for different wavelengths. If the distance $L_{\text{g-fc}}$ deviates greatly from the $r_2\cos\alpha_2$, as shown in Fig. 1(b), namely, for $L_{\text{g-fc}} \ll (\text{or} \gg) r_2\cos\alpha_2$, $\alpha_{2'}$ for the wavelength λc-$\Delta\lambda$ becomes much smaller (or larger) than α_2. Thus, in such cases, the aberrations cannot be simultaneously corrected by the same optical parameters over a wide spectral region.

3. Example of the Design

The following example is intended to illustrate the application of the modified arrangement. It is a Czerny–Turner imaging spectrometer with a fixed plane grating (300 lines/mm) and the following specifications: the effective focal length is 80 mm, $F/8$, and the slit size is 50 μm × 5 mm. The spectrometer is an UV to visible system with a wide spectral region from 0.28 to 0.68 μm. A CCD with a size of 25 mm × 25 mm (pixel size 24 μm × 24 μm) is employed. The design wavelength is the central wavelength of 0.48 μm. The system layout is sketched in Fig. 2. Here the optical system design program ZEMAX [9] is used to model and analyze this system.

With the help of ZEMAX, optical performances of the system can be predicted and plotted. Spot diagrams at the detector surface are calculated for different fields of view at the entrance slit with our modified and the existing Czerny–Turner configuration. At first, a spherical focusing mirror is used to demonstrate the expanded image that is due to the astigmatism and coma aberration is diminished on the basis of Eq. (5). In fact, the expanded image of approximately 20 μm (tangential) × 1 mm (sagittal) is obtained, as shown in Fig. 3(a). Then the toroidal focusing mirror with a radius of curvature of 368 mm along the sagittal plane was used to correct astigmatism on the basis of Eqs. (7) and (8). We obtain substantially improved images with a spot size of approximately 20 μm, which is less than 1/50 in the sagittal direction when compared with those obtained by use of the spherical mirror, as shown in Fig. 3(b). The optical parameters with respect to the aberration correction are summarized in Table 1.

To show that the best position of the grating is important to obtain excellent aberration properties over a wide spectral region, we compare the aberration properties in our modified arrangement with those in the existing arrangement. RMS spot radius is given as a function of wavelength. Obviously, when $L_{\text{g-fc}}$ is equal to $2f_{t2}$, good imaging quality is obtained over the whole wavelength region, as shown in

Table 1. Optical Parameters of the Imaging Spectrometer

	Coma-Corrected Spectrometer	Astigmatism-Corrected Spectrometer	Optimized by Ray Tracing
Specifications	at 480 nm	at 480 nm	at 480 nm
[a] i (°)	−3	−3	−3
[a] θ (°)	−11.323	−11.323	−11.323
[b] $r_1 = \rho_1$ (mm)	300	300	300
[b] r_2 (mm)	380	380	380
[b] ρ_2 (mm)	380	368	366.104
[c] α_1 (°)	5.296	5.296	5.862
[c] α_2 (°)	9	9	9
[d] $L_{\text{es-cl}}$ (mm)	149.36	149.36	149.216
[d] $L_{\text{cl-g}}$ (mm)	298.719	298.719	298.431
[d] $L_{\text{g-fc}}$ (mm)	375.322	375.322	375.322
[d] $L_{\text{fc-im}}$ (mm)	187.661	187.661	187.757

[a] i, θ: the incident and the diffraction angles to the grating substrate.

[b] r_1, ρ_1, r_2, ρ_2: the radius of curvature of the (1) collimating and (2) focusing mirrors along the sagittal (r) and tangential (ρ) planes.

[c] α_1, α_2: the incident angles for central light to the (1) collimating and (2) focusing mirrors.

[d] $L_{\text{es-cl}}$, $L_{\text{cl-g}}$, $L_{\text{g-fc}}$, $L_{\text{cd-im}}$: the distance between the entrance slit and the collimating mirror, between the collimating mirror and the grating, between the grating and the focusing mirror, and between the focusing mirror and the image plane.

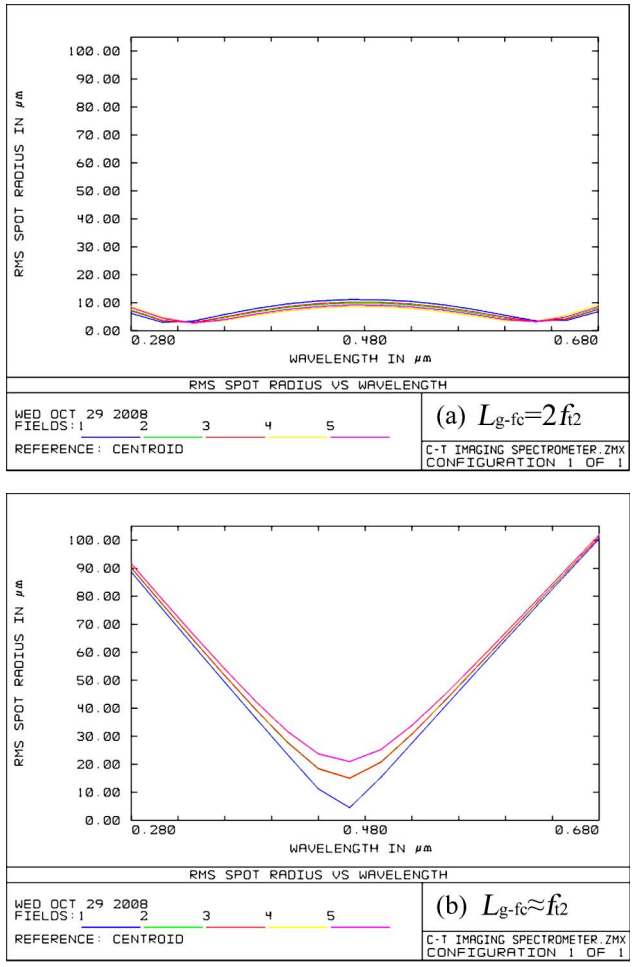

Fig. 4. (Color online) RMS spot radius versus wavelength.

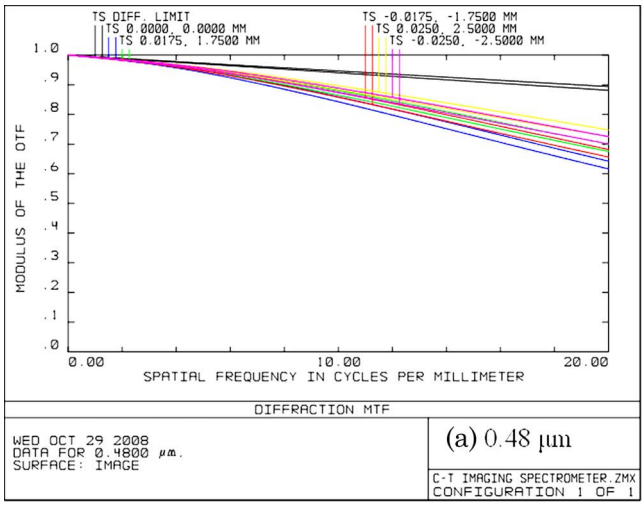

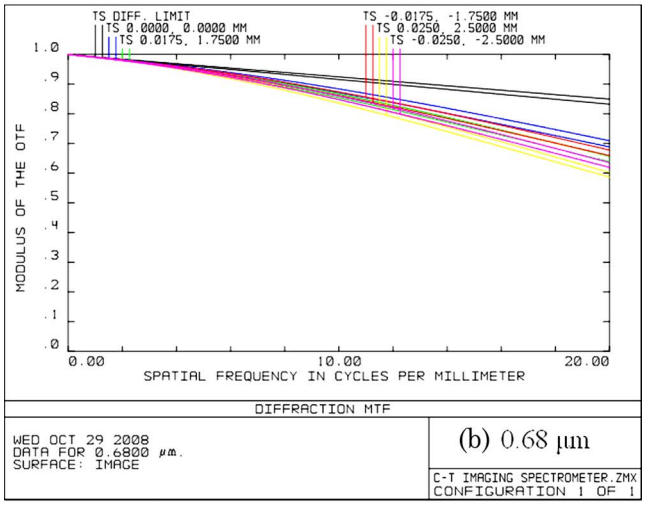

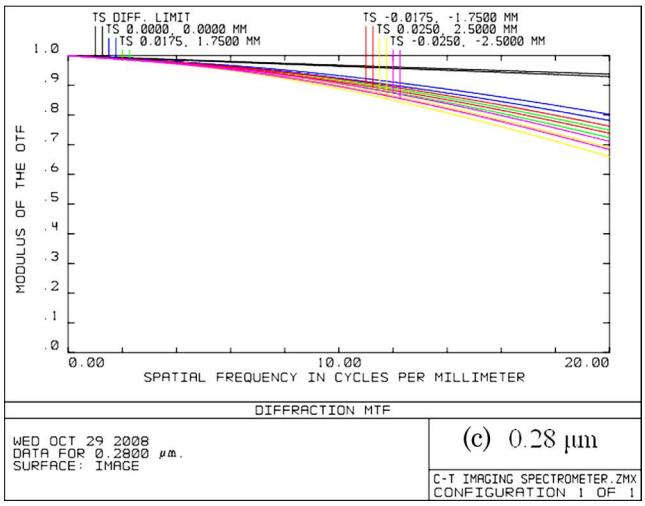

Fig. 5. (Color online) MTF of the Czerny–Turner imaging spectrometer system under central and marginal wavelengths.

Fig. 4(a). However, in the existing Czerny–Turner arrangement ($L_{g\text{-}fc} \approx f_{t2}$), good imaging quality is obtained only in the vicinity of the design wavelength (the central wavelength), as shown in Fig. 4(b).

By final optimization, we obtain excellent imaging quality at the CCD's light sensor surface. The modulation transfer function (MTF) curves are given as a function of spatial frequency in Figs. 5(a)–5(c). It is clear that the MTF of each field is larger than 0.6 at the CCD's Nyquist frequency (20 line pairs/mm) for central and marginal wavelength.

4. Summary

A variant of the Czerny–Turner arrangement that allows high-quality images to be simultaneously obtained over a wide spectral region is proposed by analyzing the dependence of aberration correction for different wavelengths. The performances of this modified Czerny–Turner arrangement are confirmed to be better than that of existing Czerny–Turner arrangements by using a practical example modeled in the optical system design program ZEMAX. The configuration is larger than the existing Czerny–Turner arrangements, but it is recommended for an imaging spectrometer with a short focal length and a wide spectral region.

The work described in this paper is supported by the National Natural Science Foundation of China (NSFC) under grant 40675083.

References and Notes

1. G. G. Chandler, "Optimization of a 4-m asymmetric Czerny–Turner spectrograph," J. Opt. Soc. Am. **58**, 895–899 (1968).
2. http//www. Jobin Yvon.com/OSD.htm.
3. R. R. Conway, M. H. Stevens, C. M. Brown, J. G. Cardon, S. E. Zasadil, and G. H. Mount, "Middle atmosphere high resolution spectrograph investigation," J. Geophys. Res. **104**, 16327–16348 (1999).
4. R. D. McPeters, S. J. Janz, E. Hilsenrath, T. L. Brown, D. E. Flittner, and D. F. Heath, "The retrieval of ozone profiles from limb scatter measurements: results from the Shuttle Ozone Limb Sounding Experiment," Geophys. Res. Lett. **27**, 2597–2600 (2000).
5. M. R. Torr and D. G. Torr, "Compact imaging spectrograph for broadband spectral simultaneity," Appl. Opt. **34**, 7888–7898 (1995).
6. M. G. Dittman, J. W. Leitch, M. Chrisp, J. V. Rodriguez, A. L. Sparks, B. K. McComas, N. H. Zaun, D. Frazier, T. Dixon, R. H. Philbrick, and D. Wasinger, "Limb broad-band imaging spectrometer for the NPOESS Ozone Mapping and Profiler Suite (OMPS)," Proc. SPIE **4814**, 120–130 (2002).
7. A. B. Shafer, L. R. Megill, and L. Droppleman, "Optimization of the Czerny–Turner spectrometer," J. Opt. Soc. Am. **54**, 879–887 (1964).
8. F. A. Jenkins and H. E. White, *Fundamental of Optics* (McGraw-Hill, 1950), p. 92.
9. ZEMAX is a trademark of Zemax Development Corporation, Bellevue, Washington 98004, USA.